Proceedings of the ASME 2009 28th International Conference on Ocean, Offshore and Arctic Engineering
OMAE2009
May 31 - June 5, 2009, Honolulu, Hawaii, USA

OMAE2009-79259

NON-LINEAR HYSTERETIC SEABED MODEL FOR CATENARY PIPELINE CONTACT

Mark Randolph
Centre for Offshore Foundation Systems
University of Western Australia, Perth

Peter Quiggin
Orcina Ltd.
Ulverston, Cumbria, UK

ABSTRACT

This paper presents a new mathematical model of the reaction force normal to the seabed, experienced by a pipeline or catenary riser in contact with the seabed. Such contact is currently often modeled using simple seabed contact models, and it is hoped that improved modeling of the seabed interaction will give more accurate predictions of system behavior, in particular for fatigue analysis.

The model uses as its primary data the pipe diameter, the seabed soil shear strength profile with depth and the soil density. Additional parameters, in particular the maximum normalized stiffness of the pipe-soil response following reversal of motion, are used to derive non-linear hyperbolic functions that model the seabed resistance force as a function of the penetration. Different functions are used for the initial penetration, for uplift and for repenetration, and the function parameters are updated each time a penetration reversal occurs. This enables the model to capture the hysteretic behavior of the seabed response and the increasing penetration of the pipe under cycles of load in the vertical plane, although no attempt is made to model softening of the soil due to remolding. The paper documents the model equations and discusses their background and characteristics. The various non-dimensional parameters of the model that are used to control the resistance response are described and their effects are illustrated.

The model is intended for use in practical engineering analysis and has been implemented in a commercial riser analysis program (Orcina 2008). The paper compares results obtained using the model against measured results for pipe-seabed interaction from laboratory and harbor experiments. It also presents results of using the model for engineering analysis of a riser under cyclic motions, and compares the resulting fatigue life with that obtained using a simple linear seabed model.

INTRODUCTION

Fatigue studies for steel catenary risers (SCRs) are typically carried out using a simple linear stiffness for the riser-seabed interaction, although there is general awareness that the appropriate stiffness will vary along the touchdown zone, depending on the amplitude of cyclic displacements (Clukey et al. 2005, 2008). The variation of stiffness with displacement amplitude is best captured by means of a non-linear soil model, avoiding the need to impose a spatially varying (fixed) stiffness through the touchdown zone. The non-linear soil model described in this paper is based on a hyperbolic secant stiffness formulation, such as those proposed by Bridge et al. (2004) and Aubeny and Biscontin (2006). Full details of the model are given later but the main features are as follows.

- The seabed normal resistance is modeled using four penetration modes, namely Not-in-Contact, Initial Penetration, Uplift and Repenetration.
- In each penetration mode the seabed reaction force per unit length, P(z), is modeled using an analytic function of the non-dimensionalized penetration z/D, where z is the penetration (pipe invert) and D is the pipe diameter.
- For each mode the analytic formulae use a term of hyperbolic form, which provides a high stiffness response for small reversals of motion, but ensures that the resistance P(z) asymptotically approaches the soil ultimate penetration resistance (for penetration) or ultimate suction resistance (for uplift), as the penetration z increases or decreases from its value when this episode of penetration or uplift started.

This model has been implemented in a riser analysis program (Orcina 2008). In later sections we compare the results of this implementation against experimental results from laboratory and harbor experiments. We also study the effect of seabed model and seabed modeling data on fatigue analysis results for an engineering analysis of a catenary pipeline. For convenience, all nomenclature is summarized below.

NOMENCLATURE

Input Data

The seabed soil model requires the following dimensional data.

- D Pipe outer diameter.
- g Acceleration due to gravity.
- s_{u0} Soil undrained shear strength at mudline.
- ρ Soil undrained shear strength gradient, i.e. the rate of change of shear strength with depth.
- ρ_{sea} Sea water density.
- ρ_{soil} Saturated soil density.

Model Parameters

The model requires a number of non-dimensional parameters that may be specified by the user. These parameters control how the soil response is modeled by the non-linear soil model.

- a, b Penetration resistance parameters of the model. These control the variation of the bearing factor $N_c(z)$ with penetration, and hence control how the ultimate penetration and suction resistance limits $P_u(z)$ and $P_{u\text{-}suc}(z)$ vary with penetration z. See Ultimate Resistance Limits below.
- f_b Soil buoyancy factor. This controls modeling of the extra buoyancy effect due to the pipe displacing soil (see Soil Extra Buoyancy Force below). Normally $f_b > 1$, to model the tendency for soil to heave locally around the pipe.
- K_{max} Normalized maximum stiffness. This controls the maximum stiffness during initial penetration, or on reversal of motion, and also how fast the resistance asymptotically approaches its limiting value.
- f_{suc} Suction resistance ratio. This controls the level of the ultimate suction (or uplift) resistance limit of the model; a higher value gives greater uplift resistance.
- λ_{suc} Normalized suction decay distance. This controls the suction uplift displacement over which suction can be maintained, by means of an exponential term multiplying $P_{u\text{-}suc}(z)$, to provide the limiting uplift resistance $P_{min}(z)$. See Uplift mode below. A lower value causes the suction resistance to decay more rapidly with uplift. A higher value causes suction to persist over greater uplift distances. This parameter also affects the repenetration limit term $P_{max}(z)$ in Repenetration mode.
- λ_{rep} Normalized repenetration offset after uplift. This controls the penetration at which the repenetration resistance limit $P_{max}(z)$ in Repenetration mode merges with the bounding curve for initial penetration resistance, $P_{IP}(z)$. A smaller value results in less penetration past the deepest point at which the pipe-soil force became negative during uplift before the response during repenetration merges with the bounding curve of initial penetration resistance. A higher value leads to greater extra penetration before the bounding curve is reached. See Repenetration Mode below.

Model Variables

A number of internal variables and functions, as listed below, are used to calculate the pipe-soil response for any given motion of the pipe.

- z Penetration of pipe invert (i.e. bottom of outer surface) below the mudline. This is the key input data to the seabed model from the structure model; the seabed model returns the seabed resistance force acting on the element and the structure model then calculates how the pipe position varies as a result.
- ζ Penetration non-dimensionalized to be in units of D/K_{max}. Therefore $\zeta = z/(D/K_{max})$.
- z_0, ζ_0, P_0 Values of z, ζ and P at which the latest episode of a given contact mode started.
- z_{max} Largest ever penetration z, for a given pipe element.
- $z_{P=0}$ Largest penetration z at which suction has started during (the deepest) uplift phase, for a given pipe element.
- $N_c(z)$ Bearing factor at penetration z.
- $s_u(z)$ Soil undrained shear strength at penetration z.
- $P_u(z)$ Ultimate penetration resistance at penetration z. This is the highest soil shear reaction force per unit length of pipe that the seabed soil can give.
- $P_{u\text{-}suc}(z)$ Ultimate suction resistance at penetration z. This is the highest uplift resistance or 'suction' force per unit length of pipe that the seabed soil can provide.
- H_{IP}, H_{UL}, H_{RP} Hyperbolic factors used in the penetration resistance formulae for initial penetration mode, uplift mode and repenetration mode, respectively.
- A_{UL}, A_{RP} Resistance ratios used within the hyperbolic factors to ensure correct initial stiffness on load reversal.
- E_{UL}, E_{RP} Exponential factors that limit uplift and repenetration resistance, to account for decay of suction with uplift movement and reduction in repenetration resistance.
- $P_{max}(z)$ Limiting resistance in repenetration mode, incorporating reduction in repenetration resistance following uplift.
- $P_{min}(z)$ Limiting suction resistance in uplift mode, incorporating decay of suction with increasing uplift displacement.
- $P(z)$ Penetration resistance at current penetration z. Together with the soil extra buoyancy force (see below) this gives the resulting pipe-soil force per unit length of pipe and thus represents the output from the model.

SEABED NON-LINEAR SOIL MODEL THEORY

Penetration Modes

The model uses 4 contact modes, as shown in Figure 1. The penetration mode of an element of a pipe is determined by its penetration, z, and in the dynamic analysis by whether the penetration has increased or decreased since the previous time step. The details are as follows.

- In the static analysis in which the initial configuration of the model is established the **Uplift** and **Repenetration** modes are not used and the penetration mode is set to

Initial Penetration if the penetration is +ve (i.e. below the seabed) or to **Not In Contact** otherwise. The effect of this is that the calculated static position assumes that any static penetration occurred as a single progressive penetration, and it does not allow for any uplift and repenetration that might have occurred during first installation.

- The dynamic simulation starts from the results of the static analysis, so each pipe element starts the simulation in either **Not In Contact** mode or **Initial Penetration** mode. If the pipe starts in **Not In Contact** mode then it changes to **Initial Penetration** mode the first time the penetration becomes +ve.
- Once initial penetration has occurred in the dynamic simulation, the pipe element then stays in **Initial Penetration** mode until it starts to lift up, and it then changes to **Uplift** mode.
- The pipe element then stays in **Uplift** mode until either the penetration falls to zero, in which case it breaks contact and changes to **Not In Contact** mode, or else until the penetration starts to increase again, in which case it changes to **Repenetration** mode. Similarly, **Repenetration** mode persists until the pipe element starts to lift up again, and it then changes to **Uplift** mode. So if the pipe element stays in contact with the seabed but oscillates up and down then it switches back and forth between **Uplift** and **Repenetration** modes.
- If the pipe element breaks contact and then later makes contact again then it enters **Repenetration** mode, *not* **Initial Penetration** mode. This is because the model assumes that second and subsequent periods of contact are made with the same area of seabed as was previously disturbed by the initial penetration.

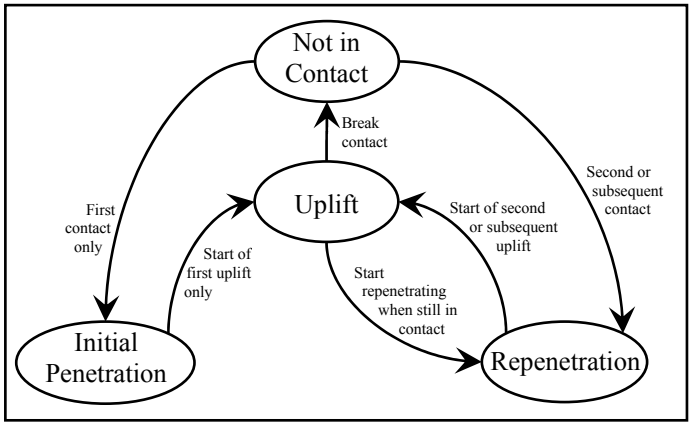

Figure 1. Soil model penetration modes

Model Characteristics

Figure 2 illustrates the model characteristics schematically, showing the variation of the pipe-soil resistance for a catenary pipeline moving up and down on the seabed. The model starts in Initial Penetration mode and gives a resistance (blue curve, see note (1) in Figure 2) that increases as the pipe penetrates the seabed, and asymptotically approaches the ultimate penetration resistance P_u (right hand dashed grey curve). This initial penetration curve (blue) is referred to as the backbone curve.

Then, when the pipe starts to lift up the model enters Uplift mode and the resistance falls (green curve, see note (2)) with an initial gradient that is controlled by K_{max}. The uplift shown in Figure 2 is sufficient that the resistance becomes negative - i.e. suction (see note (3)) and asymptotically approaches the ultimate suction resistance $P_{u\text{-}suc}$ (a proportion f_{suc} of P_u – see left hand dashed grey curve).

If the uplift continues and the pipe lifts off the seabed then the model stays in Uplift mode and the model follows the green curve further (see note (4) in Figure 2). The suction reduces as the uplift continues, and drops to zero when the penetration drops to zero. The displacement over which the suction decays, and indeed the proximity to the ultimate suction resistance curve, is controlled by λ_{suc}.

If, however, the uplift ends and repenetration starts, then the model enters Repenetration mode (purple curve, note (5) in Figure 2) and the suction rapidly falls and soon instead becomes +ve resistance. As repenetration continues the resistance rises (see note (6)) and again asymptotically approaches the ultimate penetration resistance. Repenetration following lift-off (see note (7)) follows an initially concave response, which reflects softening of the soil beneath the pipeline during uplift, before the ultimate penetration resistance is approached at a penetration just beyond the previous maximum penetration, as controlled by λ_{rep}.

Further cycles of uplift and repenetration would give further episodes of Uplift and Repenetration modes and so give hysteresis loops of seabed resistance with incremental penetration at each cycle.

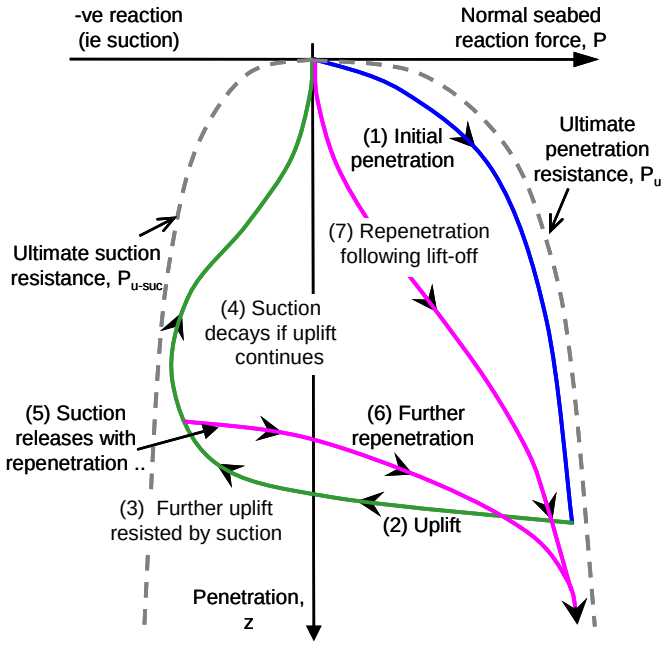

Figure 2. Soil model characteristics for different modes

Ultimate Resistance Limits

The resistance formulae are arranged so that as penetration z increases (for penetration) or decreases (for uplift) then the resistance asymptotically approaches the ultimate penetration resistance $P_u(z)$ (for penetration) or the ultimate suction resistance $P_{u\text{-}suc}(z)$ (for uplift). These ultimate penetration and suction asymptotic limits are given by

$$P_u(z) = N_c(z/D).s_u(z).D \quad (1)$$

$$P_{u\text{-}suc}(z) = -f_{suc}.P_u(z) \quad (2)$$

where

- $s_u(z)$ = undrained shear strength at penetration z $= s_{u0} + \rho.z$.
- $N_c(z/D)$ = bearing factor. For $z/D \geq 0.1$ this is modelled using the power law formula $N_c(z/D) = a.(z/D)^b$ (Aubeny et al. 2005). For $z/D < 0.1$ the formula $N_c = N_c(0.1).\sqrt{(10.z/D)}$ is used instead, which gives a good approximation to the theoretical bearing factor for shallow penetration (Randolph and White 2008a).

It should be noted that the suction resistance will depend partly on the local soil strength and partly on the pipe velocity and period of sustained uplift; use of a constant factor f_{suc} in equation (2) is therefore a simplification.

Penetration Resistance Formulae

In **Not In Contact** mode the penetration resistance P(z) is zero. In the other three modes the resistance P(z) is modeled using formulae that involve the following variables:

- $\zeta = z / (D/K_{max})$. This is the penetration, but non-dimensionalized to be in units of D/K_{max}. Essentially K_{max} is the pipe-soil stiffness, dP/dz, normalized by the ultimate net bearing pressure at that depth, P_u/D, with typical values for soft clay in the range 150 to 250 (Bridge et al. 2004, Clukey et al. 2005).
- z_0 = penetration z at which the latest episode of this contact mode started, i.e. the value at the time the latest transition into this contact mode occurred.
- $\zeta_0 = z_0 / (D/K_{max})$ = non-dimensionalized penetration at which the latest episode of this contact mode started.
- P_0 = resistance P(z) at which the latest episode of this contact mode started.

Initial Penetration Mode

For **Initial Penetration** mode the starting penetration and resistance values, z_0 and P_0, are both zero. The penetration resistance is then given by

$$P(z) = H_{IP}(\zeta).P_u(z) \quad (3)$$

where

$$H_{IP}(\zeta) = \zeta / [1 + \zeta] \quad (4)$$

The term $H_{IP}(\zeta)$ is a hyperbolic factor that equals 0 when $\zeta = 0$ when initial penetration starts, equals ½ when $\zeta = 1$, i.e. when $z = D/K_{max}$, and asymptotically approaches 1 as penetration gets large compared to D/K_{max}. The purpose of this factor is to provide a high initial stiffness ($dP/dz = K_{max}P_u/D$) while ensuring that the penetration resistance P(z) rises smoothly from zero when contact first starts (when ζ and z are both 0) and asymptotically approaches the ultimate penetration resistance, $P_u(z)$, if ζ gets large (i.e. if z gets large compared to D/K_{max}). This is illustrated by the blue curve in Figure 2, which approaches the ultimate penetration resistance limit (dashed grey curve on right) at large penetration.

Uplift Mode

For **Uplift** mode the penetration resistance is given by

$$P(z) = P_0 - H_{UL}(\zeta_0 - \zeta).(P_0 - P_{u\text{-}suc}(z)) \quad (5)$$

$$H_{UL}(\zeta_0 - \zeta) = (\zeta_0 - \zeta) / [A_{UL}(z) + (\zeta_0 - \zeta)] \quad (6)$$

$$A_{UL}(z) = (P_0 - P_{u\text{-}suc}(z)) / P_u(z_0) \quad (7)$$

but is subject to a suction limit - see later.

The term $H_{UL}(\zeta_0 - \zeta)$ is a hyperbolic factor that equals 0 when $\zeta = \zeta_0$ at the start of this uplift, and asymptotically approaches 1 if the non-dimensional uplift $(\zeta_0 - \zeta)$ gets large compared to $A_{UL}(z)$. The resistance ratio, $A_{UL}(z)$, ensures that the initial stiffness at the start of uplift is given by $K_{max}P_u(z_0)/D$. So in uplift mode the resistance given by equation (5) drops from its value P_0 when this uplift started, and asymptotically approaches the (negative) ultimate suction resistance $P_{u\text{-}suc}(z)$ if the non-dimensional uplift $(\zeta_0 - \zeta)$ gets large compared to $A_{UL}(z)$. See the green curve in Figure 2.

Experiments have shown that suction resistance can only be sustained for a limited displacement past the point where the net resistance becomes negative (Bridge et al. 2004), and the suction then decays as uplift continues. To model this the resistance given by equation (5) is limited to be no less than (i.e. no more suction than) a negative lower bound $P_{min}(z)$, given by:

$$P_{min}(z) = E_{UL}(z).P_{u\text{-}suc}(z) \quad (8)$$

$$E_{UL}(z) = \text{Exp}[\ \text{Min}(0, (z - z_{P=0}) / (\lambda_{suc}\, z_{max})\ )\ ] \quad (9)$$

Here the term $(z - z_{P=0})/(\lambda_{suc}z_{max})$ is used as a measure of uplift relative to the maximum penetration at which suction has started.

The exponent in the expression for $E_{UL}(z)$ is zero or negative, so $E_{UL}(z) \leq 1$. $E_{UL}(z)$ equals 1 when $z \geq z_{P=0}$, but decays towards zero if the penetration z is less than the largest penetration, $z_{P=0}$, at which suction has ever occurred during uplift. The effect of this is that the term $P_{min}(z)$ limits suction to be no more than $P_{u\text{-}suc}(z)$ when the first uplift starts, but as the pipe element lifts up higher (relative to the maximum penetration at which suction has ever occurred during uplift) then the suction is limited more. This models the suction decay effect observed experimentally.

Repenetration Mode

For **Repenetration** mode the penetration resistance is given by

$$P(z) = P_0 + H_{RP}(\zeta - \zeta_0).(P_u(z) - P_0) \quad (10)$$

$$H_{RP}(\zeta - \zeta_0) = (\zeta - \zeta_0) / [A_{RP}(z) + (\zeta - \zeta_0)] \quad (11)$$

$$A_{RP}(z) = (P_u(z) - P_0) / P_{u*} \quad (12)$$

but subject to a repenetration resistance upper bound - see later. In these equations:

- ζ_0 and P_0 = non-dimensional penetration and resistance at the start of this repenetration
- $P_{u*} = P_u(z)$ if $P_0 \leq 0$, i.e. if this repenetration started from a zero or negative resistance
- $P_{u*} = P_u(z^*)$ if $P_0 > 0$, where z* is the penetration when the preceding episode of uplift started.

The term $H_{RP}(\zeta - \zeta_0)$ in equation (10) is a hyperbolic factor that equals 0 when $\zeta = \zeta_0$ at the start of this repenetration, and asymptotically approaches 1 if the non-dimensional repenetration $(\zeta - \zeta_0)$ gets large compared to $A_{RP}(z)$. So the repenetration mode resistance given by equation (10) rises from its value P_0 when this repenetration starts, and asymptotically approaches the ultimate penetration resistance $P_u(z)$ if the non-dimensional repenetration $(\zeta - \zeta_0)$ gets large compared to $A_{RP}(z)$.

Experimental data from joint industry projects such as STRIDE and CARISIMA (see Bridge et al. 2004) have found that when repenetration occurs following large uplift movement the repenetration resistance is reduced until the previous maximum penetration is approached. To model this the repenetration resistance given by equation (10) is limited to an upper limit $P_{max}(z)$ given by:

$$P_{max}(z) = E_{RP}(z).P_{IP}(z) \qquad (13)$$

$$E_{RP}(z) = \text{Exp}[\text{Min}(0, (z - z_{P=0}) / (\lambda_{suc}\, z_{max}) - \lambda_{rep})] \qquad (14)$$

where $P_{IP}(z)$ is the penetration resistance that initial penetration mode would give at this penetration, as given by equation (3).

The exponent in the expression for $E_{RP}(z)$ is zero or negative, so $E_{RP}(z) \leq 1$. The expression for $E_{RP}(z)$ gives a value < 1, and so limits the repenetration resistance to be less than the ultimate penetration resistance $P_u(z)$, until the penetration z exceeds $z_{P=0}$ by a certain amount. The first term in the exponential function mimics that in the corresponding exponential for uplift resistance, and reflects the soft response observed following significant uplift displacement. The additional term, λ_{rep}, delays rejoining the limiting resistance curve until just past the previous maximum penetration, thus modeling incremental penetration of the pipe under cycles of uplift and repenetration (see purple curves in Figure 2). The magnitude of the additional penetration with each cycle is controlled by λ_{rep}, which may vary from 0 (essentially no incremental penetration) to perhaps 0.3 (nominal incremental penetration of about 0.3D).

Soil Extra Buoyancy Force

The seabed resistance formulae given above model the resistance P(z) due to the soil shear strength. In addition to this there is an extra buoyancy force due to the fact that the pipe element displaces soil that has a higher saturated density than the water. To model this the following extra buoyancy force is applied, vertically upwards, in addition to the resistance P(z).

$$\text{Extra Soil Buoyancy Force} = f_b.A_{disp}.(\rho_{soil} - \rho_{sea}).g \qquad (15)$$

where A_{disp} = displacement area = nominal area of the pipe that is below the seabed tangent plane.

The factor f_b is normally greater than 1, which models the fact that when the seabed soil is displaced it does not disperse thinly across the seabed plane, but instead tends to heave locally around the penetrating object. The effect of this is that the extra buoyancy is typically about 50 % greater than the standard theoretical buoyancy force $A_{disp}.(\rho_{soil} - \rho_{sea}).g$ that would apply if the soil was fully fluid (Randolph and White 2008b, Merifield et al. 2009).

TYPICAL VALUES FOR MODEL PARAMETERS

The non-dimensional model parameters may be considered in two groups: those where default values may be reasonably assumed; and those that users of the model will wish to adjust to suit particular conditions. The first category includes the power law coefficients (a, b) for the bearing factor, N_c, the buoyancy factor, f_b, and the normalized maximum stiffness, K_{max}.

The power law coefficients should be considered in combination, rather than as separate values, with typical combinations ranging from (5, 0.2) to (6.5, 0.3) (Aubeny et al. 2005), depending on the roughness of the pipe and the strength profile with depth. Rounded values of (6, 0.25) were suggested by Randolph and White (2008b).

The buoyancy factor, f_b, should not be taken less than unity (Archimedes principle), but a value close to 1.5 has been shown to match the results of large deformation finite element analysis of pipe penetration (Randolph and White 2008b). In most cases, the buoyancy component of resistance will be much less than the resistance from the soil, unless fully softened conditions are to be modeled, for example adopting a shear strength profile based on remolded conditions.

The normalized secant stiffness, $(\Delta P/\Delta z)/(D/P_u)$, is a measure of the effective stiffness since the last reversal in penetration or since penetration started. It has been found (Bridge et al. 2004, Aubeny et al. 2008, Clukey et al, 2008) to have the following range of values:

- 150 to 400 for cyclic displacements of ~0.1% of the pipe diameter, D
- reduced to ~100 for cyclic displacements of ~0.5% of D
- reduced to ~40 for cyclic displacements of 2.5% of D.

For the model, a maximum normalized stiffness of $K_{max} = 200$ leads to normalized secant stiffnesses of: 167 for $z/D = 0.001$ ($\zeta = 0.2$), 100 for $z/D = 0.005$ ($\zeta = 1$), and 40 for $z/D = 0.02$ ($\zeta = 4$). These values are in reasonable agreement with the experimental data quoted above.

The second group of model parameters control the maximum suction, f_{suc}, the displacement over which the suction decays, λ_{suc}, and the delay in mobilizing full resistance during repenetration, λ_{rep}.

The amount of suction resistance during uplift has been found to depend on a variety of factors, in particular the rate at which the pipe is lifted up, the length of time over which

upward motion is sustained and the recent history of cyclic motion (Bridge et al. 2004). However, given the very limited experimental data currently available, the model has adopted a specific suction resistance ratio, f_{suc}, which may be specified in the range zero to unity, although an upper limit of about 0.7 is probably realistic, even for fast uplift following a quiescent period. Evidence from the harbor tests discussed later suggests that, during cyclic motion of the pipe, the suction resistance reduces to a low level within a few cycles as the soil beneath the pipe softens (Bridge and Willis, 2002). As such, while single uplift motions of a pipe may be best modeled by values of f_{suc} between 0.5 and 1, for fatigue studies or other applications with many cycles of loading, values in the range 0 to 0.3 would be more appropriate.

The distance over which the suction resistance decays will also be affected by the rate of motion and the previous displacement history, but is typically of the order of the pipeline diameter or less. The suction decay parameter, λ_{suc}, may therefore be chosen so that the uplift resistance becomes small within an uplift displacement of about 1 diameter. Values in the range 0.2 to 0.6 are appropriate for this.

The final parameter, λ_{rep}, controls the delay in mobilizing the ultimate resistance curve during repenetration, and was introduced to allow simulation of progressive penetration with cumulative load-controlled cycles of movement. A value in the range 0.1 to 0.5 matches experimental data reasonably, as discussed later.

An example response of the model under a complex (but artificial) displacement history is shown in Figure 3, for model parameters as listed in Table 1, ignoring buoyancy effects. The response follows the general characteristics illustrated in Figure 2, in particular with high stiffness on reversal of motion direction, and asymptotic merging with limiting resistance curves following large monotonic motion. The exponential adjustment factors in equations (8)-(9) and (13)-(14) can lead to artificial step changes in gradient, as shown in the two extended repenetration curves, but these make little difference to the overall response of the pipeline in practical applications.

Table 1. Model parameters for example in Figure 3

Parameter	Symbol	Value
Pipe diameter	D	0.35 m
Mudline shear strength	s_{u0}	5 kPa
Shear strength gradient	ρ	1.5 kPa/m
Power law parameter	a	6
Power law parameter	b	0.25
Normalized maximum stiffness	K_{max}	200
Suction ratio	f_{suc}	0.6
Suction decay parameter	λ_{suc}	0.4
Repenetration parameter	λ_{rep}	0.2

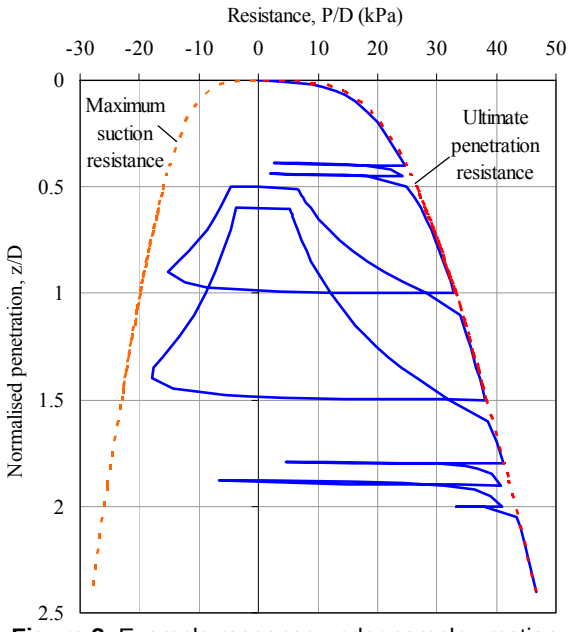

Figure 3. Example response under complex motion

COMPARISON WITH MODEL TESTS

The performance of the model has been evaluated by comparing results of the OrcaFlex implementation of the model against model test results reported by Aubeny et al. (2008), where a small pipe segment, 25 mm diameter by 125 mm long, was penetrated into a pre-consolidated kaolin sample on the laboratory floor. The shear strength in the kaolin was measured using a T-bar penetrometer, and showed essentially uniform strength with depth, with $s_u \sim 3.6$ kPa at the depth of primary interest (2 pipe diameters).

Three tests were reported, referred to as 'monotonic', 'small amplitude cyclic' and 'large amplitude cyclic' tests. The backbone penetration curves from the monotonic and large amplitude cyclic tests were very similar, and formed the basis from which the numerical model parameters were chosen, while the small amplitude cyclic test gave slightly lower penetration resistance. The three tests, together with the numerical simulation of the monotonic test, are shown in Figure 4 and the model parameters are summarized in Table 2.

In the small amplitude cyclic test, the pipe was first penetrated to about 2 diameters under a net pressure (P/D) of 21 kPa, and then subjected to 10 cycles of net pressure between 14.6 and 21 kPa, 10 cycles between 8.2 and 21 kPa, and 100 cycles between 2 and 21 kPa. For the model parameters in Table 2, a larger pressure (of 24.5 kPa) was needed to penetrate the pipe to the starting depth, but thereafter the numerical simulation gave a reasonable match to the test data, although with slightly greater incremental penetration (see Figure 5)

Table 2. Parameters for model tests in kaolin

Parameter	Symbol	Value
Pipe diameter	D	0.025 m
Mudline shear strength	s_{u0}	3.56 kPa
Shear strength gradient	ρ	0 kPa/m
Power law parameter	a	6
Power law parameter	b	0.2
Normalized maximum stiffness	K_{max}	250
Suction ratio	f_{suc}	0.7
Suction decay parameter	λ_{suc}	0.7
Repenetration parameter	λ_{rep}	0.4

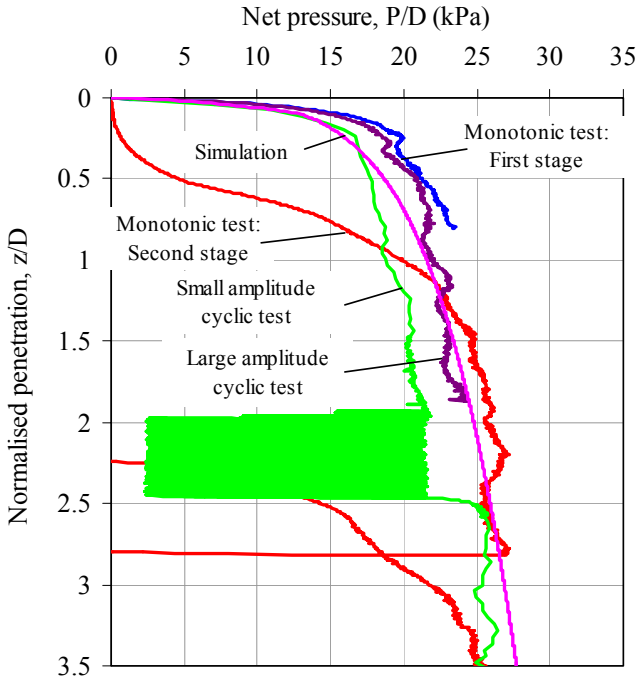

Figure 4. Simulation of monotonic response from model tests of Aubeny et al. (2008)

In the large amplitude cyclic test, the pipe was first penetrated to 2 diameters, and then subjected to 30 cycles of uplift by 1 diameter, followed by repenetration to a net pressure of 20 kPa (Aubeny et al. 2008). The corresponding simulation is shown in Figure 6, and matches the test data very well, although with more abrupt changes in gradient of the cyclic load-penetration curves than shown by the model tests.

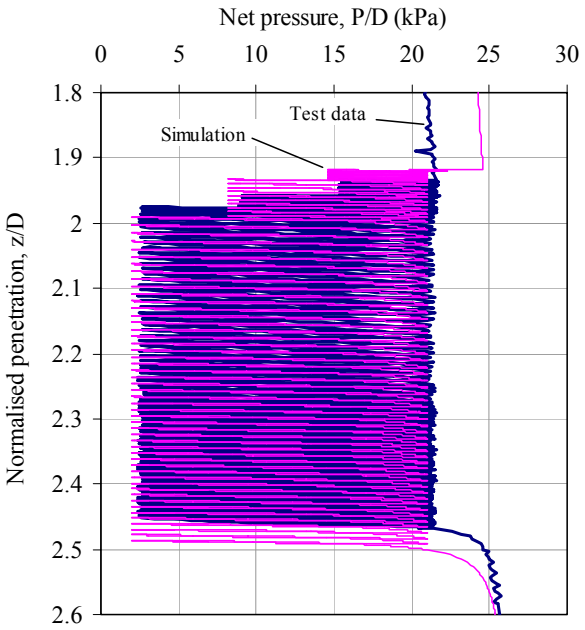

Figure 5. Simulation of small amplitude cyclic test

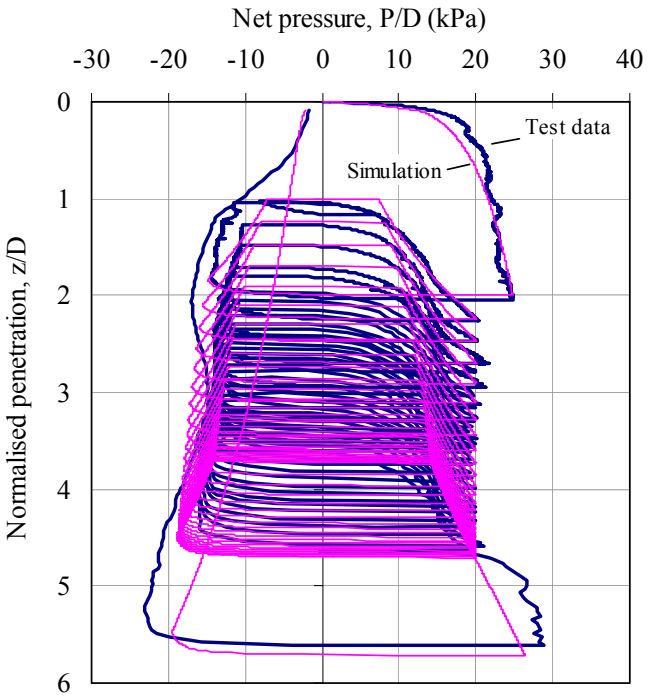

Figure 6. Simulation of large amplitude cyclic test

COMPARISON WITH WATCHET HARBOR TESTS

Bridge et al. (2004) reported results from full scale tests of catenary touchdown of a fully-instrumented riser, performed in Watchet harbor, UK. The tests studied the bending moment and tension as the touchdown point (TDP) moved due to top end motion, and amongst other things the results showed significant

evidence of suction effect as the riser was lifted away from the seabed after a period of rest.

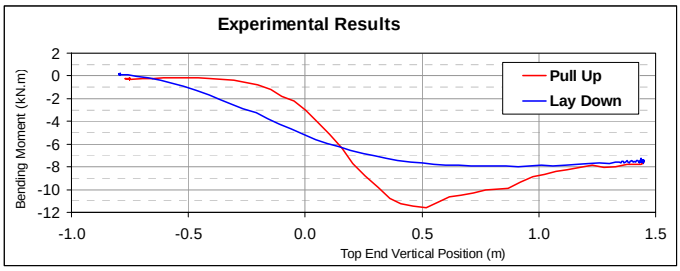

Figure 7. Measured bending moment during pull-up and lay down

Two of the Watchet tests that showed large suction effect consisted of raising the top of the riser at 0.1m/s for 22s (test 2-10, pull-up) followed by lowering the top end again at the same velocity (test 2-11, lay down). This process lifted a section of the riser off the seabed during the pull-up and then laid it down again. Figure 7 shows the measured bending moment at a strain gage (gage D) near the centre of the lifted section, as a function of the top end vertical position.

Negative bending moments correspond to sag bend, so the bending moment falls during the pull-up as the TDP passes the gage point, and then rises again as the TDP passes back through as the riser is laid back down again. The results show significant suction effect, since during pull-up the bending moment drops to -11.5 kNm as the TDP passes the gage point, but then rises again once the gage point is clear of the seabed. By contrast, during lay down the bending moment simply rises as the gage point is laid down onto the seabed and the riser at that point therefore straightens.

These tests have been modeled in OrcaFlex using the non-linear soil model, and the results are shown in Figure 8. The soil data and model parameters used for these calculations are given in Table 3.

Table 3. Parameters for Watchet test

Parameter	Symbol	Value
Pipe diameter	D	0.1683 m
Mudline shear strength	s_{u0}	0 kPa
Shear strength gradient	ρ	6 kPa/m
Power law parameter	a	6
Power law parameter	b	0.25
Normalized maximum stiffness	K_{max}	300
Suction ratio	f_{suc}	1.0
Suction decay parameter	λ_{suc}	2.0
Repenetration parameter	λ_{rep}	0.3

The calculated results also show evidence of the suction that the model gives, but the calculated results using the soil model show significantly less suction effect than the Watchet results from tests 2-10 and 2-11. However other Watchet pull-up tests, e.g. cyclic tests where the seabed was remolded, showed much less suction effect. Also, the magnitude of suction during uplift is affected by the rate of pull-up, as noted by Bridge et al. (2004). At the moment the non-linear soil model described above does not account for rate effects, and it is thought that this is why the soil model does not match the level of suction measured in tests 2-10 and 2-11 of the Watchet harbor tests.

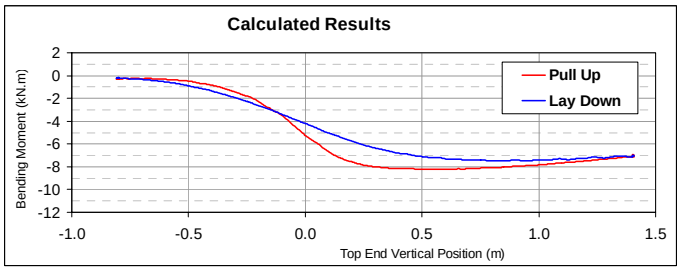

Figure 8. Calculated bending moment during pull-up and lay down

EFFECT ON FATIGUE ANALYSIS

Seabed response is considered to have a significant effect on the fatigue damage near touchdown of a catenary riser. To study this a series of fatigue analyses were performed for a deepwater catenary riser, using different seabed models and seabed data.

The case used for these fatigue analyses was a 9 inch steel catenary riser, 1 inch wall thickness, with submerged weight of 1.01 kN/m and bending stiffness, EI, of 17.7 MNm^2. The riser was 1600 m long and hung in 1000 m water depth from the pontoon of a semi-submersible platform, with a mean departure angle of 10° from the downward vertical. A flexjoint with linear stiffness 10 kNm/deg was used at the top end connection of the riser to the platform, and riser touchdown was at approximately 1200m arc length from the top. The environmental loads applied to the system comprised 30 storms, representing a condensed Gulf of Mexico irregular wave scatter table. In all cases the environment was applied in the plane of the riser, from anchor towards hang-off.

Fatigue analyses were first undertaken for this case using a simple linear seabed model, with a range of values of linear stiffness. The effect of the seabed stiffness on the predicted fatigue life is shown in Figure 9. The effect is significant; higher seabed stiffness gave lower predicted fatigue life.

Further fatigue analyses were then undertaken, but using the non-linear soil model with a range of values of the mudline shear strength and two different levels of the suction resistance ratio f_{suc}. The soil data and model parameters used are given in Table 4 and the predicted fatigue life is shown in Figure 10, as a function of the mudline shear strength. As with the linear seabed model, higher mudline shear strength, which corresponds to a stiffer seabed, gives higher predicted damage and lower fatigue life.

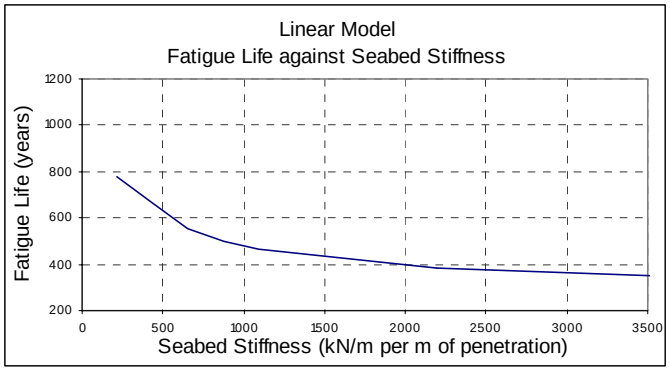

Figure 9. Linear seabed model :
Stiffness effect on predicted fatigue life

Table 4. Non-linear Model parameters for Fatigue Analyses

Parameter	Symbol	Value
Pipe diameter	D	0.228 m
Mudline shear strength	s_{u0}	0 to 3.5 kPa
Shear strength gradient	ρ	1.3 kPa/m
Power law parameter	a	6
Power law parameter	b	0.25
Normalized maximum stiffness	K_{max}	200
Suction ratio	f_{suc}	0.2 and 0.6
Suction decay parameter	λ_{suc}	1.0
Repenetration parameter	λ_{rep}	0.3

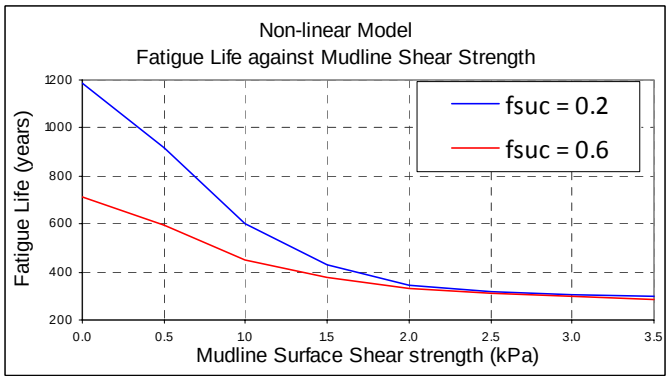

Figure 10. Non-linear soil model :
Mudline shear strength effect on predicted fatigue life

Finally, further fatigue analyses were undertaken using the non-linear soil model, but this time with a range of values of shear strength gradient, in order to study the effect of shear strength gradient on fatigue. For these analyses the mudline shear strength s_{u0} was set to zero and the suction resistance ratio f_{suc} was set to 0.2, but the other soil data and model parameters used were the same as in the previous analyses (as given Table 4). The predicted fatigue life is shown in Figure 11 as a function of the shear strength gradient.

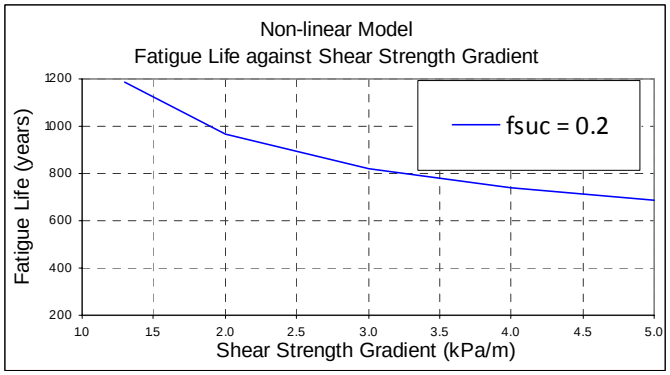

Figure 11. Non-linear soil model :
Shear strength gradient effect on predicted fatigue life

The results from these fatigue analyses confirm that the seabed resistance characteristics have a significant effect on fatigue damage, and that stiffer seabed conditions and greater suction effects should be expected to give higher damage. This reinforces the importance of trying to improve the accuracy of seabed modeling in riser analysis work.

CONCLUSIONS

This paper has presented a relatively simple non-linear seabed model that captures the essence of varying soil stiffness with the magnitude of pipeline penetration and cyclic motions. A hyperbolic response is used to capture the critical aspects of (a) high stiffness on reversal of movement direction and for small cyclic displacements, and (b) asymptotic behavior with limiting penetration and uplift resistance following large downward or upward movements.

The model allows the user to adjust the amount of suction resistance during uplift, and the displacement over which the suction is sustained. Incremental penetration of the pipe under cycles of movement may also be simulated. The model was validated against laboratory and field-scale experiments with reasonable accuracy shown.

The influence of the seabed stiffness and soil model on the fatigue life was demonstrated by a parametric study using both linear and non-linear soil models. The significance of the degree of suction assumed, and also the strength intercept at the mudline, was also shown.

ACKNOWLEDGEMENTS

This work forms part of the activities of the Centre for Offshore Foundation Systems (COFS), established under the Australian Research Council's Research Centres Program and now supported by the State Government of Western Australia as a Centre of Excellence. The soil model described here was developed in a collaborative venture between COFS and Orcina Ltd in the UK.

REFERENCES

Aubeny, C.P., Shi, H. and Murff, J.D. (2005). Collapse loads for a cylinder embedded in trench in cohesive soil. Int. J. Geomechanics, ASCE (2005) 5(4), 320–325.

Aubeny, C.P. and Biscontin, G. (2006). Seafloor interaction with steel catenary risers. Offshore Technology Research Center, Texas A&M University, College Station, Houston, Final Project Report to Minerals Management Service, OTRC Library Number 9/06A173.

Aubeny, C., Gaudin, C. and Randolph, M.F. (2008). Cyclic tests of model pipe in kaolin. Proc. Offshore Technology Conf., Houston, Paper OTC 19494.

Bridge, C., Laver, K., Clukey, E., Evans, T. (2004). Steel catenary riser touchdown point vertical interaction models. Proc. Offshore Technology Conf., Houston, Paper OTC 16628.

Bridge, C. and Willis, N. (2002). Steel catenary risers – results and conclusions from large scale simulations of seabed interaction. Proc. 14th Annual Conf. on Deep Offshore Technology.

Clukey, E.C., Haustermans, L., and Dyvik, R. (2005). Model tests to simulate riser-soil interaction effects in touchdown point region. Proc. Int. Symp. on Frontiers in Offshore Geotechnics - ISFOG, Perth, Australia, 651-658.

Clukey, E.C., Young, A.G., Dobias, J.R. and Garmon, G.R. (2008). Soil response and stiffness laboratory measurements of SCR pipe/soil interaction. Proc. Offshore Technology Conf., Houston, Paper OTC 19303.

Merifield, R., White, D.J. and Randolph, M.F. (2009). The effect of surface heave on the response of partially-embedded pipelines on clay. J. of Geotechnical and Geoenvironmental Engineering, ASCE (accepted October 2008).

Orcina (2008), OrcaFlex User Manual, www.orcina.com, UK.

Randolph, M.F. and White, D.J. (2008a). Upper bound yield envelopes for pipelines at shallow embedment in clay. Géotechnique, 58(4), 297-301.

Randolph, M.F. and White, D.J. (2008b). Pipeline embedment in deep water: processes and quantitative assessment. Proc. Offshore Technology Conf., Houston, Paper OTC 19128.